Accepted Manuscript

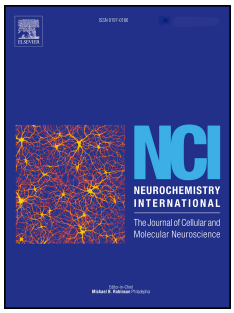

A tryptamine-paeonol hybridization compound inhibits LPS-mediated inflammation in BV2 cells

Eun-Hye Jung, Ji-Sun Hwang, Mi-Youn Kwon, Kyung-Hong Kim, Hyeongjin Cho, In Kyoon Lyoo, Sujeong Shin, Jeong-Ho Park, Inn-Oc Han

PII: S0197-0186(16)30270-4

DOI: 10.1016/j.neuint.2016.08.010

Reference: NCI 3909

To appear in: *Neurochemistry International*

Received Date: 28 March 2016

Revised Date: 2 August 2016

Accepted Date: 23 August 2016

Please cite this article as: Jung, E.-H., Hwang, J.-S., Kwon, M.-Y., Kim, K.-H., Cho, H., Lyoo, I.K., Shin, S., Park, J.-H., Han, I.-O., A tryptamine-paeonol hybridization compound inhibits LPS-mediated inflammation in BV2 cells, *Neurochemistry International* (2016), doi: 10.1016/j.neuint.2016.08.010.

A Tryptamine-paeonol Hybridization Compound Inhibits LPS-mediated Inflammation in BV2 Cells

Eun-Hye Jung[1], Ji-Sun Hwang[1], Mi-Youn Kwon[1], Kyung-Hong Kim[1], Hyeongjin Cho[2], In Kyoon Lyoo[3], Sujeong Shin[4], Jeong-Ho Park[4*], Inn-Oc Han[1*]

[1]Department of Physiology and Biophysics, College of Medicine, [2]Department of Chemistry, Inha University, Incheon, Korea, [3]Ewha Brain Institute, Department of Brain and Cognitive Sciences, College of Pharmacy, Ewha Womans University, Seoul, Korea, [4]Department of Chemical & Biological Engineering, Hanbat National University, Daejeon, Korea

Running title: Anti-inflammatory effects of tryptamine-paeonol hybridization compounds

There is no potential conflict of interest in this paper.

[*]To whom correspondence should be addressed.
Inn-Oc Han, Ph.D.
Departmentof Physiology and Biophysics, College of Medicine,
Inha University, 100 Inha Ro, Nam-Gu, Incheon, 22212 Korea.
Tel: (82) 32-890-0924, Fax: (82) 32-890-0647

E-mail: iohan@inha.ac.kr

ABSTRACT

In the present study, we synthesized and evaluated the anti-inflammatory effects of three tryptamine (Trm) hybrid compounds, HBU-375, HBU-376 and HBU-379. The Click reaction between the azido-Trm and 2- or 4-propazylated paeonol moiety resulted in HBU-376 and HBU-375, respectively. HBU-379 was generated by hybridizing Trm with propazylated acetyl-syringic acid. HBU-376 and HBU-375 dose-dependently inhibited LPS and caused nitric oxide (NO) generation in BV2 cells, whereas HBU-379 minimally inhibited NO generation, indicating that the paeonol unit plays an important role in the anti-inflammatory effect of Trm hybrid compounds. Although HBU-375 and HBU-376 demonstrated a similar inhibitory effect on LPS-induced NO generation, HBU-376 resulted in less cellular toxicity presumably due to the free phenolic hydroxyl group of paeonol. Therefore, HBU-376 may be a promising anti-inflamamtory agent conferring minimal cytotoxicity. HBU-376 significantly and dose-dependently inhibited LPS-induced NO products, NO synthase (iNOS), cyclooxygenase-2 (COX-2), interleukin-6, MCP-1 and interleukin-1β mRNA expressions and iNOS and COX-2 protein expressions. However, at the same concentrations, Trm or paeonol individually did not inhibit LPS-mediated production of inflammatory molecules. HBU-376 inhibited both LPS-induced STAT-3 phosphorylation and nuclear factor-kappa B (NF-κB) activation. Furthermore, LPS-mediated DNA binding of c-Rel, p50 and p52 to the NF-κB binding site of the iNOS promoter was inhibited by HBU-376, whereas Trm and paeonol did not inhibit LPS-induced NF-κB activation and DNA binding of c-Rel, p50 and p52. Overall, our data suggest that the Trm-paeonol hybrid compound down-regulates inflammatory responses by inhibiting NF-κB and

NF-κB-dependent gene expression. This suggests that it is a potential therapeutic agent for inflammatory diseases of the central nervous system.

INTRODUCTION

Two chemical entities, when joined covalently, could have properties other than or more prominent than those expected from each of the individual components. This concept has been successfully employed in drug development in the creation of hybrid drugs (Decker, 2011) (Meunier, 2008). Two chemically distinct pharmacophores being combined into one molecule by a linker results in the hybrid molecules potential behaving in two ways. When combined in a metabolically labile way, the pharmacophores can act as mutual prodrugs (Noh *et al.*, 2015). The pharmacophores combined through a metabolically stable linker suggests the hybridization can be a mutual derivatization including pharmacologically significant chemical entities rather than just structural diversification (Fortin *et al.*, 2013). In these regards, hybridization can potentially synergize and amplify the effects of the individual drug components.

Tryptamine (Trm) is an indole alkaloid widely distributed in fungi, plants, and animals. Endogenous tryptamines include serotonin (5-hydroxytryptamine) and melatonin (N-acetyl-5-methoxytryptamine) and are believed to play neuromodulator or neurotransmitter roles. Furthermore, tryptamines are known to confer a wide variety of biological effects, including anticancer, antimicrobial to anti-inflammatory effects (Kaushik et al., 2013; Mollica et al., 2012). Several studies reported that melatonin exhibits a neuroprotective effect and an anti-inflammatory effect of the brain through the anti-inflammatory function on the microglia (Tsai *et al.*, 2011; Ding *et al.*, 2014). Furthermore, melatonin attenuates lipopolysaccharide (LPS)-stimulated inflammation of astrocytes (Niranjan *et al.*, 2012),

demonstrating its anti-neuroinflammatory function. However, few studies have been focused on the direct effect of melatonin or Trm on LPS-induced regulation of pro-inflammatory genes in cultured microglial cells.

Paeonol (2'-hydroxy-4'-methoxyacetophenone) is an important component of herbs of the Paeonia genus. These herbs have been used as drugs in traditional oriental medicine for a long time. Paeonol has a wide range of pharmacological functions, including anti-oxidative, anti-inflammatory and neuroprotective activities (Hsieh *et al.*, 2006; Lin *et al.*, 2015). In particular, the anti-inflammatory properties of paeonol have been well demonstrated in macrophages and endothelial cells (Nizamutdinova *et al.*, 2007; Huang *et al.*, 2008). More recently, it has been described that paeonol attenuates LPS-stimulated microglial inflammation in the BV2 cell line (Himaya *et al.*, 2012; Nam *et al.*, 2014).

Inflammation in the central nervous system is immensely consequential in the pathogenesis of neurodegenerative disorders such as stroke, traumatic injury, Parkinson's disease, and Alzheimer's disease. The aim of this study was to determine the anti-inflammatory effect of Trm-paeonol hybrid compounds on LPS-induced inflammation in BV2 microglia with minimum cytotoxicity. The potential benefits of the hybrid drug approach were pursued by combining the two chemical units, Trm and paeonol, which possess potent anti-inflammatory activities. Collectively, the current results suggest that paeonol may be a potential neuroprotective agent which inhibits microglia-mediated inflammation and oxidative stress.

MATERIALS AND METHODS

Reagents

Except where otherwise noted, all reagents were purchased from Sigma Chemical Company (St. Louis, MO).

Synthesis of HBU-375, HBU-376 and HBU-379

3-(2-azidoethyl)-1H-indole (**1**). Tryptamine (600 mg, 3.75 mmol) was dissolved in MeOH (10 mL). Then imidazole sulfonyl azide (648 mg, 3.75 mmol) and K_2CO_3 (518 mg, 3.75 mmol) were added to the solution. The mixture was stirred at room temperature for 12hr. After the reaction was completed, 10 mL H_2O was added to the reaction mixture. The mixture was extracted with DCM (10 mL x 3). The combined organic layer were washed with brine, dried over $MgSO_4$, and concentrated under reduced pressure. The crude product was purified by silica gel column chromatography (Ethyl acetate : Hexane = 3 : 1) to give compound **1** (240 mg, 40% yield).

IR (KBr, v, cm^{-1}): 3413 (amine), 2091 (azide); ^1H NMR ($CDCl_3$, 400 MHz) δ 3.05 (t, *J*=7.6 Hz, 2H), 3.55 (t, *J*=7.2 Hz, 2H), 7.04 (s, 1H), 7.12 (t, *J*=8.8 Hz, 1H), 7.20 (t, *J*=8.2 Hz, 1H), 7.34 (d, *J*=7.6 Hz, 1H), 7.57 (d, *J*=8 Hz, 1H), 7.98 (s, 1H)

1-(2-hydroxy-4-(prop-2-yn-1-yloxy)phenyl)ethanone (**2**). A 25mL round-bottomed flask was charged with 2,4-dihydroxy acetophenone (1.15 g, 7.57 mmol), cesium carbonate (0.82 g, 2.52 mmol) and acetone (10 mL). Propargyl bromide (0.22 mL, 2.52 mmol) was then added to the reaction mixture. The mixture was stirred at room temperature for 24hr. After the reaction was completed, 10 mL H_2O was added to the reaction mixture. The mixture was extracted with DCM (10 mL x 3). The combined organic layer were washed with brine, dried

over $MgSO_4$, and concentrated under reduced pressure. The crude product was purified by silica gel column chromatography (Ethyl acetate : Hexane = 1 : 6) to give compound **2** (860 mg, 50% yield).

^{1}H NMR ($CDCl_3$, 400 MHz) δ 2.52 (s, 1H), 2.53 (s, 3H), 4.68 (s, 2H), 6.47 (dd, *J*=9.6 Hz, *J*=2.4 Hz, 1H), 6.48 (d, *J*=2.4 Hz, 1H), 7.62 (d, *J*=2.4 Hz, 1H), 7.62 (d, *J*=9.6 Hz, 1H), 12.66 (s, 1H); ^{13}C NMR ($CDCl_3$, 100 MHz) δ 26.19, 55.89, 76.50, 77.61, 102.01, 107.68, 114.42, 132.42, 163.73, 164.83, 202.76

1-(4-methoxy-2-(prop-2-yn-1-yloxy)phenyl)ethanone (**3**). To the solution of paeonol (2.0 g, 12.04 mmol) and cesium carbonate (7.85 g, 24.08 mmol) in acetone (15 mL), propargyl bromide (1.04 mL, 14.45 mmol) was then added to the reaction mixture. The mixture was stirred at room temperature for 24hr. After the reaction was completed, 10 mL H_2O was added to the reaction mixture. The mixture was extracted with DCM (10 mL x 3). The combined organic layer were washed with brine, dried over $MgSO_4$, and concentrated under reduced pressure. The crude product was purified by silica gel column chromatography (Ethyl acetate : Hexane = 1 : 4) to give compound **3** (2.33 g, 95% yield).

^{1}H NMR ($CDCl_3$, 400 MHz) δ 2.53 (s, 1H), 2.59 (s, 3H), 3.86 (s, 3H), 3.86 (s, 3H), 4.79 (s, 2H), 6.41 (d, *J*=2.4 Hz, 1H), 6.51 (dd, *J*=8.8 Hz, *J*=2.2 Hz, 1H), 7.80 (d, *J*=8.8 Hz, 1H); ^{13}C NMR ($CDCl_3$, 100 MHz) δ 31.97, 55.60, 56.25, 76.28, 77.77, 99.74, 106.16, 121.76, 132.77. 158.86. 164.26. 197.54

2,6-Dimethoxy-4-(prop-2-yn-1-ylcarbamoyl)phenyl acetate (**4**). Acetyl syringic acid (900 mg, 1.26 mmol), DMAP (225 mg, 0.13 mmol) and EDC (255 mg, 1.39 mmol) were

dissolved in DCM (5 mL). The reaction mixture was cooled to 0^{o}C. Propargyl amine (81 μL, 1.26 mmol) was then added to the reaction mixture. After the reaction was completed, 10 mL H_2O was added to the reaction mixture. The mixture was extracted with DCM (10 mL x 3). The combined organic layer were washed with brine, dried over $MgSO_4$, and concentrated under reduced pressure. The crude product was purified by silica gel column chromatography (DCM : MeOH = 19 : 1) to give compound **4** (280 mg, 80% yield).

^{1}H NMR ($CDCl_3$, 400 MHz) δ 2.27 (t, *J*=2.4 Hz, 1H), 2.33 (s, 3H), 3.84 (s, 6H), 4.21 (q, *J*=2.4 Hz, 2H), 6.32 (bs, 1H), 6.98 (s, 2H)

1-(4-((1-(2-(1H-indol-3-yl)ethyl)-1H-1,2,3-triazol-4-yl)methoxy)-2-hydroxyphenyl)ethanone (HBU-375). Compound **1** (160 mg, 0.87 mmol) and Compound **2** (150 mg, 0.79 mmol) was dissolved in acetone (5 mL). To the reaction mixture $Cu(PPh_3)_3Br$ (73 mg, 0.079 mmol) was added. The reaction mixture was carried out the Click reaction by using *Microwave Synthesizer Biotage*® at 65℃ for 30min. After the reaction was completed, the solvent was evaporated. The crude product was purified by silica gel column chromatography (DCM : MeOH = 19 : 1) to give compound HBU-**375** (287 mg, 79% yield).

Melting point: 117℃; ^{1}H NMR (DMSO, 400 MHz) δ 2.52 (s, 3H), 3.22 (t, *J*=6.8 Hz, 2H), 4.60 (t, *J*=8 Hz, 2H), 5.15 (s, 2H), 6.54 (d, *J*=11.6 Hz, 1H), 6.57 (s, 1H), 6.93(t, *J*=8 Hz, 1H), 7.02 (t, *J*=8 Hz, 1H), 7.04 (s 1H), 7.28 (d, *J*=8 Hz, 1H), 7.48 (d, *J*=7.6 Hz, 1H), 7.80 (d, *J*=8.8 Hz, 1H), 8.20 (s, 1H), 10.81 (s, 1H), 12.57 (s, 1H); ^{13}C NMR (DMSO, 100 MHz) δ 26.4, 27.1, 50.5, 62.0, 102.1, 180.1, 110.4, 111.9, 114.4, 118.6, 118.9, 121.5, 123.6, 125.2, 127.3, 133.8, 136.6, 152.2, 164.4, 164.9, 203.7; ESI-HRMS: [MH]+ 377.0 (calcd 377.41).

1-(2-((1-(2-(1H-indol-3-yl)ethyl)-1H-1,2,3-triazol-4-yl) methoxy)-4-methoxyphenyl) ethanone (HBU-376). HUB-**376** (340 mg, 92% yield) was synthesized by using compound **1** (220 mg, 1.08mmol) and **3** (200 mg, 0.98 mmol) by the same procedure as the synthesis of HBU-**375**.

Melting point: 108℃; ^{1}H NMR (DMSO, 400 MHz) δ 2.35 (s, 3H), 3.26 (t, *J*=7.6 Hz, 2H), 3.81 (s, 3H), 4.65 (t, *J*=6.8 Hz, 2H), 5.26 (s, 1H), 6.59 (d, *J*=8.4 Hz, 1H), 6.85 (s, 1H), 6.94 (t, *J*=2.4 Hz, 1H), 7.01 (s, 1H), 7.02 (t, *J*=2.4 Hz, 1H), 7.31 (d, *J*=4 Hz, 1H), 7.50 (d, *J*=8 Hz, 1H), 7.60 (d, *J*=4 Hz, 1H), 7.62 (d, *J*=8.8 Hz, 1H), 8.21 (s, 1H), 10.82 (s, 1H) ; ^{13}C NMR ($CDCl_3$, 100 MHz) δ 26.62, 32.00, 50.89, 55.67, 62.21, 99.50, 106.14, 110.53, 111.71, 118.08, 119.53, 121.36, 122.18, 123.00, 123.72, 126.67, 132.57(2C), 136.42, 159.61, 164.50, 198.11; ESI-HRMS: [MH]+377.41 (calcd 377.2).

N-((1-(2-(1H-indol-3-yl)ethyl)-1H-1,2,3-triazol-4-yl)methyl)-4-hydroxy-3,5-dimethoxybenzamide (HBU-379). HUB-**379** (226 mg, 70% yield) was synthesized by using compound **1** (220 mg, 1.08mmol) and **4** (170 mg, 0.72 mmol) by the same procedure as the synthesis of HBU-**375**.

Melting point: 170 ℃; ^{1}H NMR (DMSO, 400 MHz) δ 2.20 (s, 3H), 3.19 (s, 2H), 3.75 (s, 6H), 4.45 (s, 2H), 4.54 (s, 2H), 6.90 (s, 1H), 7.00 (s, 1H), 7.05 (s, 1H), 7.21 (s, 1H), 7.26 (s, 2H), 7.46 (s, 1H), 7.97 (s, 1H), 9.01 (s, 1H), 10.79 (s, 1H) ; ^{13}C NMR (DMSO, 100 MHz) δ 20.59, 26.46, 35.44, 50.44, 56.56(2C), 104.68(2C), 104.76, 110.48, 111.83, 118.91, 121.50, 123.56, 127.32, 130.66, 132.61, 136.56, 151.95(2C), 165.72, 168.21(2C); ESI-HRMS: [MH]+ 421.5 (calcd 421.5)

LogD values for HBU-375, HBU-376 and HBU-379 were calculated by using

Discovery Studio program (Accelrys, San Diego, CA).

Cell Cultures

Murine BV2 microglial cell line has been used as a suitable model for *in vitro* studies of activated microglia (Kim *et al.*, 2004) cells. BV2 microglia, RAW264.7 macrophage, and N2a neuroblastoma cells were maintained at 37°C at 5% CO_2 in Dulbecco's modified Eagle's medium (DMEM) supplemented with 10% FBS (Hyclone, Logan, Utah), streptomycin and penicillin.

Cell Viability

Cell viability was measured by 3-[4,5-dimethylthiazol-2-yl]-2,5-diphenyltetrasolium bromide (MTT) as described previously (Hwang *et al.*, 2010). In brief, BV2 or N2a cells were seeded to each well of 24-well plates at the density of 5 x 10^4 cells/well. After 24 h, cells were stimulated with LPS (100 ng/ml) and/or HBU-375, HBU-376 and HBU-379 for 24 or 48 h. MTT solution (50 μl) was added to each well, and the plates were incubated in the dark for 4 h at 37ºC. Formazan crystals were dissolved by of solution of DMSO:EtOH=1:1. Absorbance at 595 nm was read on a microplate reader, and the results were expressed as a % of control (untreated).

Nitrite Measurement

Nitrite level, an index for NO production, was measured in the supernatant of BV2 cells by the Griess method (Hwang *et al.*, 2010). Cells were seeded to each well of 24-well plates at the density of 5x 10^4 cells/well. After 24 h, cells were stimulated with LPS (100

ng/ml) and/or HBU compounds. Nitrite accumulation in the culture medium was measured at various time points by adding equal volumes of Griess reagent (1% sulphanilamide, 0.1% naphthylenediamine 5% phosphoric acid) and samples of medium. The optical density at 550 nm (OD 550) was measured with a microplate reader. Sodium nitrite, diluted in culture medium at concentrations of 10–100 µM, was used to generate a standard curve.

RT-PCR and quantitative real-time PCR

Total RNA from BV2 cells was extracted with TRIzol^{TM} (Invitrogen, Carlsbad, CA). RNA samples were reverse-transcribed into cDNA using SuperScript II. PCR was performed using specific primers of mouse described below. Gene expression values were compared with the housekeeping gene GAPDH. PCR reaction contained a total volume of 15 µl containing 1.5 mM magnesium chloride ($MgCl_2$), 250 µM deoxy-nucleoside triphosphate, 1.25 units Taq DNA polymerase, 10 picomoles of primer, and 25 ng cellular DNA templates. The PCR products were electrophoresed in 1 % agarose gel in Tris/Borate/EDTA (TBE) buffer. The gels were observed and taken pictures using UV imaging equipment.

The expressions of mRNAs were quantitatively determined by measuring incorporation of fluorescent SYBR green into double-stranded DNA (iCycleriQ, Bio-Rad). Relative mRNA levels were calculated from the PCR profiles of each sample using the threshold cycle (Ct), corresponding to the cycle at which a statistically significant increase in fluorescence occurred. Ct is considered the amount of template present in the starting reaction. To correct for differences in the amount of total cDNA in the starting reaction, Ct values for an endogenous control (input DNA) were subtracted from those of the corresponding sample.

All real-time PCR data presented are the results of two independent DNA preparations and amplifications.

PCR primers used in this study (mouse)

	Forward Primer	Reverse Primer
iNOS	ACTTCCGAGTGTGGAACTCG	TGGCTACTTCCTCCAGGATG
COX-2	GCTGTACAAGCAGTGGCAAA	GTCTGGAGTGGGAGGCACT
IL-1β	GGAGAAGCTGT GGCAGCTA	GCTGATGTACCAGTTGGGGA
IL-6	CCGGAGAGGAGACTTCACAG	TGGTCTTGGTCCTTAGCCAC
TNF-α	GACCCTCACACTCAGATCAT	TTGAAGAGAACCTGGGAGTA
MCP-1	GTCCCTGTCATGCTTCTGGG	GAAGACCTTAGGGCAGATGCAG
GAPDH	TCATTGACCTCAACTACATGGT	CTAAG CAGTTGGTGGTGCAG

Immunoblotting

Total cell protein was prepared by lysing the cells in buffer (10 mM Tris, 140 mM NaCl, 1% Triton, 0.5 % SDS and protease inhibitors, pH 8.0). Prepared protein samples (20 μg protein each) were separated by SDS-PAGE and transferred to Hybond^{TM}-ECL^{TM} nitrocellulose membranes (Amersham Biosciences, Piscataway, NJ). All of the antibodies used were from Santa Cruz Biotechnology (Santa Cruz, CA), except antibodies against iNOS (BD Biosciences, San Jose, CA), Cox-2 (Cayman Chemicals, Ann Arbor, Mi), glyceraldehyde 3-phosphate dehydrogenase (GAPDH) (Cell Signaling Technology, Danvers, MA), ERK1/2 (Cell Signaling Technology), p-JNK (Invitrogen), JNK (Cell Signaling Technology), p-P38 (Cell Signaling Technology), and α-tubulin (Calbiochem, Darmstadt,

Germany). The membrane was incubated with antibodies for overnight at 4°C. After washing with TBST (50 mM Tris, 150 mM NaCl and 0.05% Tween 20, pH 7.6), the membrane was incubated in a buffer containing HRP-conjugated secondary antibodies (1:10,000 dilution in TBST) for 1 h at room temperature. The protein bands were detected using an ECL detection reagent (Amersham Biosciences).

Streptavidin-agarose pull-down assay

Biotin pull-down assays were performed as described previously, with minor modifications (Hwang *et al.*, 2010). The procedure allows for quantitative binding of transactivators or molecules of interest to a specific probe: a 20-nucleotide sequence containing the NF-κB binding site (5'-GCTAGGGGGATTTTCCCTCT-3') at position -957/-977 of the iNOS promoter. Two complementary DNAs were synthesized and biotinylated by Bioneer Corporation (Korea) and annealed to generate a double-stranded probe. Binding assays were performed by incubating 500 μg nuclear protein extracts with 2 μg biotinylated DNA probe and 25 μl streptavidin-conjugated agarose beads for 1 h. DNA-protein complexes were analyzed by Western blotting using the indicated antibodies.

Transfection and NF-κB reporter gene assay

The NF-κB reporter (Clontech, Mountain View, CA) contained three copies of the κB-binding sequence fused to the firefly luciferase gene. RAW 264.7 cells in 12 well culture plate (5 x 10^5/well) were transfected with Lipofectamine Plus. Luciferase activity was assayed 24 h after transfection and normalized to transfection efficiency using a cotransfected β-galactosidase plasmid. Bioluminescence was measured using a

TurnerDesigns luminometer (TD-20/20).

Electrophoretic Mobility Shift Assay (EMSA)

Nuclear protein extracts were prepared as described previously (Hwang *et al.*, 2013) The double-stranded DNA oligonucleotide probe containing the consensus NF-κB binding site (Promega, Madison, WI) was labeled by polynucleotide kinase (New England Biolabs, Beverly, MA) and purified through Sephadex G-25 spin columns. Aliquots of nuclear protein (20 μg) were incubated with labeled oligonucleotides in binding buffer (50 mM KCl, 12.5 mM HEPES pH 7.6, 6.25 mM $MgCl_2$, 0.05 mM EDTA, 0.5 % Nonidet P-40, 0.5 mM DTT, 5% glycerol and 2 μg poly-[dI-dC]) for 30 min on ice. The reaction samples were separated on 4.5% polyacrylamide gel containing 2% glycerol, and the gel was electrophoresed at 200 V at room temperature for 1.5 h. The gel was then dried and exposed to x-ray film (Kodak, Rochester, NY) with an intensifying screen at -80°C.

Statistical Analysis

Data are expressed as the mean ± standard deviation (S.D., error bars) of 3 independent experiments. Statistical comparison of the re results was carried out using one-way analysis of variance (ANOVA), followed by Tukey's post hoc test for data analysis. A p value <0.05 was considered as statistically significant.

RESULTS

Synthesis of a hybrid compound HBU-375, HBU-376 and HBU-379

Molecular hybridization employed the Click reaction which gave rise to a triazole moiety as a linker between tryptamine and paeonol (Kolb *et al.*, 2001). We prepared azido tryptamine (**1**), a 4-propazylated paeonol derivative (**2**), a 2-propazylated paeonol derivative (**3**), and acetyl propazyl syringic amide (**4**), as described in 'Materials and Methods' (Fig. 1A). Next, we synthesized HBU-375, -376 and -379 by the Click reaction (Fig. 1B).

Structures of the prepared compounds were verified by nuclear magnetic resonance (NMR) and mass spectrometry (MS) analyses. Lipophilicity is an important factor controlling the interaction of drugs with biological membranes. Generally, sufficient absorption of an orally administered drug can be obtained when the logD value is greater than 2; the logD values (aqueous solubility at pH 7.4) of HBU-375, -376 and -379 are 3.489, 3.716 and 2.952, respectively (data not shown). Therefore HBU-375, -376 and -379 are potentially highly permeable to cells.

Cell cytotoxicity of HBU-376, -375 and -379 was compared

We examined the cell cytotoxicity of HBU-375, -376 and -379 in BV2 cells utilizing MTT assays. HBU-376 did not significantly change cell viability up to 20 μM but induced cytotoxicity in higher than 30 μM concentrations at 24 h (Fig. 2A, upper panels). The propazylated paeonol-compound, HBU-375, was more toxic; it induced significant cell death at 10 μM at 24 h. The propazylated syringic acid-compound, HBU-379, did not induce cell death up to concentrations of 50 μM. Control compounds, Trm, paeonol, dihydroxy acetonphenone or syringic acid did not influence cell viability up to 50 μM (Fig. 2A, lower

panels). Cytotoxic effects of HBU-375, -376 and -379 were also examined in N2a murine neuroblastoma cells and demonstrated no significant toxic effect up to 30 μM.

Anti-inflammatory effects of HBU-375, HBU-376 and HBU-379 were compared

We compared the anti-inflammatory effects of the three different Trm hybrid compounds with propazylated paeonol, paeonol or propazylated syringic amide, HBU-375, HBU-376 and HBU-379, respectively. BV2 cells were treated with the indicated concentrations of HBU-376, -375 or -379 or their control compounds, Trm, paeonol, dihydroxy acetonphenone or syringic acid for 2 h prior to stimulation with LPS (100 ng/ml) for 24 h. LPS-induced nitrite production was specifically suppressed by HBU-376 and -375, but not by other compounds (Fig. 3). Accordingly, hybridization between Trm with a paeonol unit specifically inhibits LPS-induced NO generation. Same concentrations of melatonin, an endogenous Trm-based compound, did not effect on LPS-induced NO generation in BV2 cells (data not shown).

Anti-inflammatory effect of HBU-376, Trm and paeonol were examined

The effect of HBU-376, Trm and paeonol on LPS-induced nitrite production was assessed. BV2 cells were treated with the indicated concentrations of HBU-376, Trm or paeonol for 2 h prior to stimulation with LPS (100 ng/mL). LPS robustly induced nitrite release at 24 h and further increased at 48 h as previously described (Hwang *et al.*, 2013). This increase was suppressed by HBU-376 in a dose-dependent manner (Fig. 4A). However, the same concentrations of Trm or paeonol did not inhibit LPS-induced nitrite production in BV2 cells. Morphological examinations under a microscope indicated that LPS caused

activation-induced cell death at 48 h. HBU-376 significantly protected against activation-induced cell death (Fig. 4B) whereas Trm or paeonol yielded no protection.

HBU-376 inhibits the upregulation of pro-inflammatory molecules at the mRNA and protein levels

We examined the effects of HBU-376 on LPS-induced expression of inflammatory genes that have been reported to be induced by the LPS-induced inflammatory response in microglia. Stimulation of BV2 cells with LPS (100 ng/ml) induced the expression of iNOS and COX-2 at 24 h. HBU-376 inhibited the expression of iNOS and COX-2 protein to a lesser extent in a dose-dependent manner in BV2 cells (Fig. 5A), while the same doses of Trm or paeonol were ineffective. Furthermore, 25 μM HBU-376, inhibited LPS-induced iNOS, COX-2, IL-6, TNF-α, IL-1β and MCP-1 mRNA expression were measured by RT-PCR (Fig. 5B) and quantitative real time PCR for iNOS COX-2 and IL-6 (Fig. 5C) in BV2 cells at 24 h. However, the same dose of Trm or paeonol did not inhibit the mRNA levels of inflammatory molecules.

HBU-376 suppresses LPS-induced STAT-3 phosphorylation and NF-κB activation

We next examined the effect of HBU-376 on the activation of MAPKs, STAT and NF-κB, the major signaling proteins involved in the regulation of the expression of the inflammatory mediators in response to LPS in microglia. 376, Trm or paeonol did not influence LPS-induced phosphorylation of ERK1/2, p38 or JNK at 30 min and 6 h. However, HBU-376, but not Trm or paeonol, significantly inhibited basal and LPS-induced STAT-3 phosphorylation at 6 h (Fig. 6A). Next, we examined the effect of HBU-376, Trm or paeonol

on NF-κB activation. LPS-induced IκB-α phosphorylation and IκB-α degradation were not significantly changed by HBU-376, Trm or paeonol (Fig. 6A). Instead, LPS-mediated activation of NF-κB luciferase reporter activity was markedly suppressed by HBU-H376 but not by Trm or paeonol (Fig. 6B). The inhibitory regulation of NF-κB by HBU-376 was confirmed by electrophoretic mobility shift assays (EMSAs); HBU-376 significantly reduced LPS-induced DNA binding of NF-κB (Fig. 6C). Trm slightly inhibited NF-κB activation whereas paeonol yielded no such inhibitory effect. Between the two NF-κB sites in the mouse iNOS promoter, the distal NF-κB site (-957/-977) is important for a LPS response. To determine whether HBU-376 influences LPS-induced binding of NF-κB/Rel family proteins (p65, p50 and c-Rel) to this site, we assayed the ability of these proteins to bind to a biotinylated oligonucleotide corresponding to the distal NF-κB site in the iNOS promoter. LPS increased the DNA bindings of p65 and c-Rel at 30 min and bindings of p65, c-Rel, p105/50 and p100/p52 at 6 h. HBU-376 inhibited the DNA-binding properties of c-Rel, p50 and p52, whereas Trm or paeonol resulted in no effect (Fig. 6D).

DISCUSSION

In this study, we compared the effects of three different tryptamine (Trm) hybrid compounds, HBU-375, -376, and -379, on the inflammatory responses of BV-2 microglial cells activated by lipopolysaccharide (LPS). We further explored the underlying working mechanisms HBU-376. Although HBU-375 demonstrated a similar anti-inflammatory effect compared to HBU-376 for LPS-induced NO generation, it was more cytotoxic than HBU-376 in BV2 cells. A hydroxyl group (—OH) in paeonol of HBU-375 which bonds directly to an aromatic hydrocarbon group is called a phenol and phenolic compounds normally act as antioxidants. However, the product generated after the anti-oxidation reaction or the autoxidation of phenolic compounds has sometimes resulted in cell death. Therefore, HBU-376 may qualify as a better compound employed an anti-inflammatory drug. In addition, in order to access the importance of the paeonol group for anti-inflammatory activity, HBU-379 was generated and evaluated for its anti-inflammatory effect. HBU-379 was clearly ineffective. HBU-379 is synthesized by hybridizing Trm with syringic acid instead of paeonol or its derivative in HBU-376 or HBU-375. Paeonol has been considered a promising neuroprotective or anti-neurodegenerative compound due to its anti-inflammatory and free-radical scavenging properties (Ruimi *et al.*, 2010; Lin *et al.*, 2015). In particular, a recent report indicates that paeonol inhibits LPS plus interferon-gamma (IFN-γ)-mediated iNOS/NO generation in BV2 microglial cells. However, in our experiment, paeonol did not inhibit LPS-induced iNOS/NO generation up to 50 μM. This inconsistent result may reflect that the characteristics of stimulation, which is LPS instead of LPS plus IFN-γ, may stimulate a distinct signaling pathway to be inhibited by paeonol. Otherwise, minor differences in compound preparation or the culture condition might result in a different effect of paeonol for NO/iNOS induction in BV2 cells. Discrepancies in responses between LPS and LPS plus

IFN-γ on the inhibitory effect of paeonol remain to be elucidated. However, the importance of our work implies that the hybrid compound presented a potent anti-inflammatory effect in concentration ranges where paeonol itself was ineffective. Since tryptamine derivatives, such as N-acetyl-5-methoxytryptamine (melatonin) or 5-hydroxytryptamine (serotonin) exhibited anti-inflammatory function in the brain, hybridization between tryptamine and paeonol to generate a novel anti-inflammatory compound may be considered as a valuable neuroprotective agent.

LPS stimulation includes the phosphorylation of p38 mitogen-activated protein kinases (MAPKs), extracellular signal-regulated kinase (ERK)-1/2, and c-Jun NH_2-terminal kinase (JNK), leading to the activation of NF-κB in macrophages. MAPKs and NF-κB are important regulators of various genes involved in immune and inflammatory responses, including iNOS and COX-2 (Xie *et al.*, 1994). HBU-376 exhibited a suppressive effect on LPS-induced NF-κB activation but was ineffective on LPS-induced MAPKs activation, suggesting that the inhibition of NF-κB activity is independent of MAPKs. HBU-376 inhibited LPS-induced DNA binding of c-Rel, p52 and p50 to NF-κB sites in the iNOS promoter at 24 h. HBU-376 may inhibit protein interactions of c-Rel with p50 or p52 in order to recruit them onto the iNOS promoter. Otherwise, HBU-376 may reduce the DNA binding affinity of NF-κBs by either activation of inhibitory factors or changed posttranslational modifications. The detailed inhibitory mechanism remains elusive yet HBU-376 represents an excellent candidate for agents of various inflammatory diseases including neurodegenerative diseases, arthritis, sepsis, cancer, obesity, and diabetes all through the inhibition of NF-κB associated gene products.

HBU-376 inhibited LPS-mediated activation of the STAT-3 phosphorylation. The JAK-STAT signal pathway plays myriad pivotal roles in immune and inflammatory responses (Kim *et al.*, 2006), suggesting that NF-κB regulates the STAT activation. In has been shown that cytokine mixture treatment activates STAT3 and STAT1 and this activation is dependent on MAPKs and NFκB signaling (Tyagi *et al.*, 2012). Therefore, HBU-376 potentially inhibited LPS-stimulated NF-κB activation and subsequently reduced downstream STAT3 activation. We observed that inhibition of JAK/STAT signaling moderately reduced iNOS expression, whereas inhibition of NF-κB in turn, inhibited STAT3 activation and completely suppressed iNOS induction in response to LPS in BV2 cells (data not shown). These results indicate that STAT3 might be one of several downstream targets of NF-κB which regulates iNOS transcription.

This report asserts a potential drug for inflammatory diseases through the design of novel combinations of natural compounds for functional, therapeutic objectives. The combination of appropriate pharmacophores into one compound has been developed to efficiently discover promising drug candidates. The well-described anti-oxidant nature of paeonol and the immunomodulatory effect of Trm derivatives led us to design a new anti-inflammatory compound by combining these molecules. We found that Trm or paeonol demonstrated little inhibitory activity against LPS-induced iNOS/NO production in BV2 cells, while HBU-376 and HBU-375 potently inhibited LPS-mediated NO production (> 90% reduction compared to the LPS-treated control). HBU-376 yielded no significant toxic effects up to 20 μM whereas HBU-375 demonstrated significant cytotoxicity at higher than 10 μM. Accordingly, HBU-376 could potentially be used to treat neurodegenerative or other

inflammation-related diseases, either alone or as an adjunct to enhance the efficacy and/or reduce the required doses of other disease-modifying immunotherapies.

AKNOWLEDGEMENT

This research was supported by the Brain Research Program through the National Research Foundation of Korea (NRF) funded by the Ministry of Science, ICT & Future Planning (2015M3C7A1028373).

REFERENCES

Decker M (2011). Hybrid molecules incorporating natural products: applications in cancer therapy, neurodegenerative disorders and beyond. Curr Med Chem 18**:** 1464-1475.

Ding K, Wang H, Xu J, Lu X, Zhang L, Zhu L (2014). Melatonin reduced microglial activation and alleviated neuroinflammation induced neuron degeneration in experimental traumatic brain injury: Possible involvement of mTOR pathway. Neurochem Int 76**:** 23-31.

Fortin S, Berube G (2013). Advances in the development of hybrid anticancer drugs. Expert Opin Drug Discov 8**:** 1029-1047.

Himaya SW, Ryu B, Qian ZJ, Kim SK (2012). Paeonol from Hippocampus kuda Bleeler suppressed the neuro-inflammatory responses in vitro via NF-kappaB and MAPK signaling pathways. Toxicol In Vitro 26**:** 878-887.

Hsieh CL, Cheng CY, Tsai TH, Lin IH, Liu CH, Chiang SY, et al. (2006). Paeonol reduced cerebral infarction involving the superoxide anion and microglia activation in ischemia-reperfusion injured rats. J Ethnopharmacol 106**:** 208-215.

Huang H, Chang EJ, Lee Y, Kim JS, Kang SS, Kim HH (2008). A genome-wide microarray analysis reveals anti-inflammatory target genes of paeonol in macrophages. Inflamm Res

57**:** 189-198.

Hwang SY, Hwang JS, Kim SY, Han IO (2013). Glucosamine inhibits lipopolysaccharide-stimulated inducible nitric oxide synthase induction by inhibiting expression of NF-kappaB/Rel proteins at the mRNA and protein levels. Nitric Oxide 31**:** 1-8.

Hwang SY, Shin JH, Hwang JS, Kim SY, Shin JA, Oh ES, et al. (2010). Glucosamine exerts a neuroprotective effect via suppression of inflammation in rat brain ischemia/reperfusion injury. Glia 58**:** 1881-1892.

Kim HS, Ye SK, Cho IH, Jung JE, Kim DH, Choi S, et al. (2006). 8-hydroxydeoxyguanosine suppresses NO production and COX-2 activity via Rac1/STATs signaling in LPS-induced brain microglia. Free Radic Biol Med 41**:** 1392-1403.

Kim WK, Hwang SY, Oh ES, Piao HZ, Kim KW, Han IO (2004). TGF-beta1 represses activation and resultant death of microglia via inhibition of phosphatidylinositol 3-kinase activity. J Immunol 172**:** 7015-7023.

Kolb HC, Finn MG, Sharpless KB (2001). Click Chemistry: Diverse Chemical Function from a Few Good Reactions. Angew Chem Int Ed Engl 40**:** 2004-2021.

Lin C, Lin HY, Chen JH, Tseng WP, Ko PY, Liu YS, et al. (2015). Effects of paeonol on anti-neuroinflammatory responses in microglial cells. Int J Mol Sci 16**:** 8844-8860.

Meunier B (2008). Hybrid molecules with a dual mode of action: dream or reality? Acc Chem Res 41**:** 69-77.

Nam KN, Woo BC, Moon SK, Park SU, Park JY, Hwang JW, et al. (2014). Paeonol attenuates inflammation-mediated neurotoxicity and microglial activation. Neural Regen Res 8**:** 1637-1643.

Niranjan R, Nath C, Shukla R (2012). Melatonin attenuated mediators of neuroinflammation and alpha-7 nicotinic acetylcholine receptor mRNA expression in lipopolysaccharide (LPS) stimulated rat astrocytoma cells, C6. Free Radic Res 46**:** 1167-1177.

Nizamutdinova IT, Oh HM, Min YN, Park SH, Lee MJ, Kim JS, et al. (2007). Paeonol suppresses intercellular adhesion molecule-1 expression in tumor necrosis factor-alpha-stimulated human umbilical vein endothelial cells by blocking p38, ERK and nuclear factor-kappaB signaling pathways. Int Immunopharmacol 7**:** 343-350.

Noh J, Kwon B, Han E, Park M, Yang W, Cho W, et al. (2015). Amplification of oxidative stress by a dual stimuli-responsive hybrid drug enhances cancer cell death. Nat Commun 6**:** 6907.

Su SY, Cheng CY, Tsai TH, Hsiang CY, Ho TY, Hsieh CL (2010). Paeonol attenuates H(2)O(2)-induced NF-kappaB-associated amyloid precursor protein expression. Am J Chin Med 38**:** 1171-1192.

Tsai MC, Chen WJ, Tsai MS, Ching CH, Chuang JI (2011). Melatonin attenuates brain contusion-induced oxidative insult, inactivation of signal transducers and activators of transcription 1, and upregulation of suppressor of cytokine signaling-3 in rats. J Pineal Res 51**:** 233-245.

Tyagi A, Agarwal C, Dwyer-Nield LD, Singh RP, Malkinson AM, Agarwal R (2012). Silibinin modulates TNF-alpha and IFN-gamma mediated signaling to regulate COX2 and iNOS expression in tumorigenic mouse lung epithelial LM2 cells. Mol Carcinog 51**:** 832-842.

Xie QW, Kashiwabara Y, Nathan C (1994). Role of transcription factor NF-kappa B/Rel in induction of nitric oxide synthase. J Biol Chem 269**:** 4705-4708.

FIGURE LEGENDS

Figure 1. The chemical structure of tryptamine (Trm), paeonol, propazylated paeonol, propazylated syringic acid, HBU-375, HBU-376 and HBU-379

HBU-375, -376, -and -379 were synthesized from Trm and paeonol or propazylated paeonol as described in Materials and Methods.

Figure 2. Cytotoxic effects of HBU-376, -375 and -379 on BV2 cells

BV2 microglia (A) or N2a (B) cells were treated with the indicated concentrations of HBU-376, -375 and -379 for 24 h. The same concentrations of control compounds, Trm, paeonol, dihydroxyacetophenone or syringic acid, were treated on BV2 cells for 24 h. Cell viability was determined using MTT assays, and the results are expressed as percentages compared to the untreated control. * represents significant differences from untreated control.

Figure 3. Examination of LPS-induced nitrite production by HBU-376, -375 and -379 in BV2 cells

BV2 cells were pre-treated with the indicated concentrations of dopamine, HBU-376, -375, -379, Trm, paeonol, dihydroxyacetophenone or syringic acid for 2 h and stimulated with 0.1 μg/ml LPS. Nitrite levels in the culture medium were measured at 24 h. * represents significant differences from the LPS-treated control.

Figure 4. Suppression of LPS-induced nitrite production and cell death by HBU-376

BV2 cells were pre-treated with the indicated concentrations of HBU-376, Trm, or paeonol (25 μM) for 2 h and stimulated with 0.1 μg/ml LPS. (A) Nitrite levels in culture medium

were measured at 24 h. (B) The phenotypes of control, HBU-376, Trm, or paeonol (25 μM each) treated cells, with or without LPS, were observed using a phase-contrast microscope at 48 h. * represents significant differences from the LPS-treated control at 24 h and ** denotes significant difference from the LPS-treated control at 48 h. Cell phenotypes are representative of 3 independent experiments.

Figure 5. Inhibition of LPS-induced pro-inflammatory molecules by HBU-376

BV2 cells were pre-treated with the indicated concentrations of HBU-376, Trm, or paeonol (25 μM) for 2 h and then treated with 0.1 μg/mL LPS for 24 h. (A) iNOS, COX-2 and GAPDH protein levels were measured by Western blotting. (B) Total RNA was prepared, and the mRNA levels of iNOS, COX-2, IL-6, TNF-α, IL-1β and MCP-1 were determined using RT-PCR. GAPDH mRNA served as a control. (C) mRNA levels for iNOS, COX-2 and IL-6 were measured by quantitative real-time PCR. * represents significant differences from the LPS-treated control. Western blots and RT-PCR results are representative of 3 independent experiments.

Figure 6. Inhibition of LPS-induced activation of NF-κB and STAT-3 phosphorylation by HBU-376

(A) BV2 cells were pretreated with HBU-376, Trm, or paeonol (25 μM) for 2 h and then treated with 0.1 μg/mL LPS. Total cell lysates were prepared at 30 min or 6 h, and the levels of phosphorylated-ERK1/2, -p38, -JNK, -STAT3, -IκB-α, and their total proteins levels along with α-tubulin levels were evaluated by Western blotting using specific antibodies. (B) RAW264.7 cells were transfected with a NF-κB-luciferase reporter plasmid. Cells were

treated with dopamine HBU-376, Trm, or paeonol (25 μM) and/or LPS (0.1 mg/ml), and luciferase activity (relative light units (RLU)), was measured at 24 h. (C~ D) BV2 cells were pre-treated with 25 μM HBU-376, Trm, or paeonol for 2 h followed by 0.1 μg/mL LPS. Nuclear extracts were prepared at 30 min and DNA binding to a ^{32}P-labeled NF-κB probe was measured by EMSA (C). Nuclear extracts were prepared at 30 min or 6 h. The binding of Rel proteins to the iNOS promoter-derived, biotinylated NF-κB probe was measured by streptavidin-agarose pull-down assays, followed by Western blotting for p65, c-Rel, p50 and p52 (D). Nuclear extract (NE) input represents 2% nuclear extract for biotin-NF-κB precipitation. B, C, and D are representative of 3 independent experiments. * denotes significant differences from the LPS-treated control.

Figure 1

A

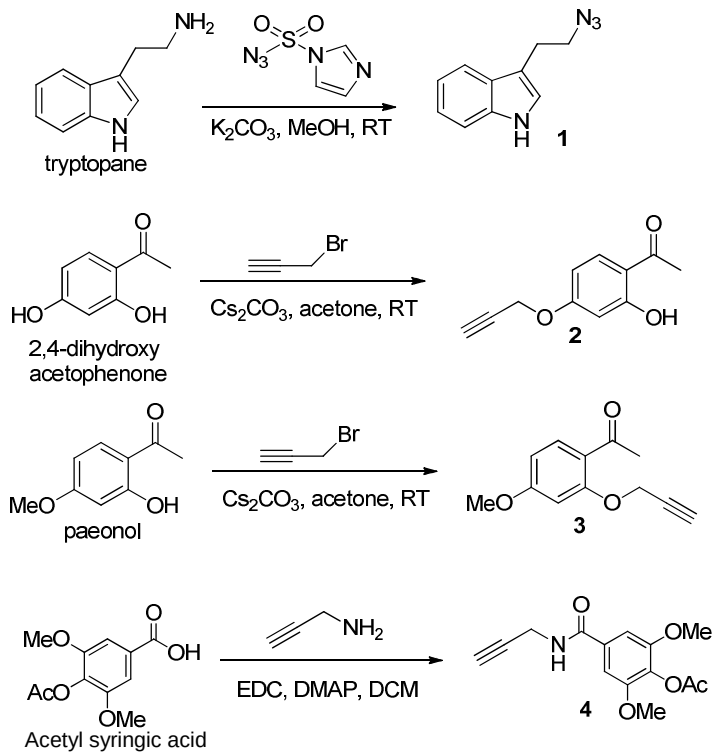

B

1	tryptamine
2	4-propazylated paeonol derivative
3	propazylated paeonol derivative
4	acetyl propazyl syringic amide)

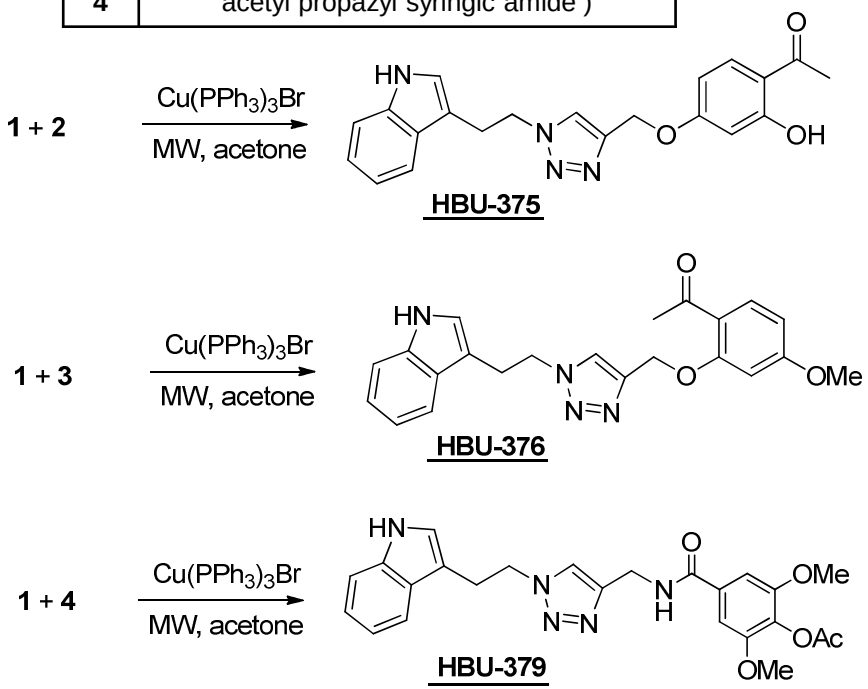

Figure 2

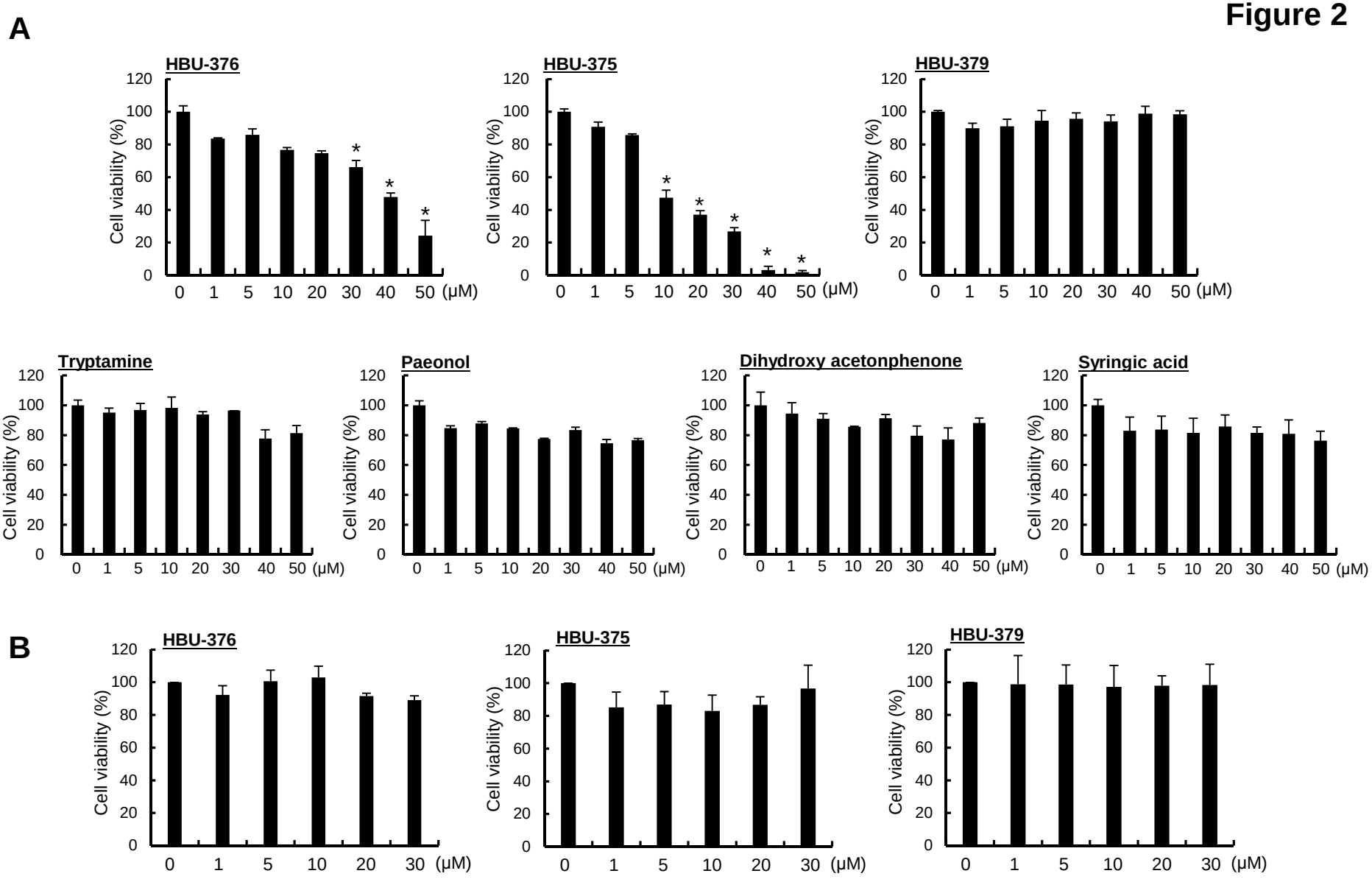
A
HBU-376
HBU-375
HBU-379
Tryptamine
Paeonol
Dihydroxy acetonphenone
Syringic acid
Cell viability (%)
0 1 5 10 20 30 40 50 (μM)
B
HBU-376
HBU-375
HBU-379
0 1 5 10 20 30 (μM)

Figure 3

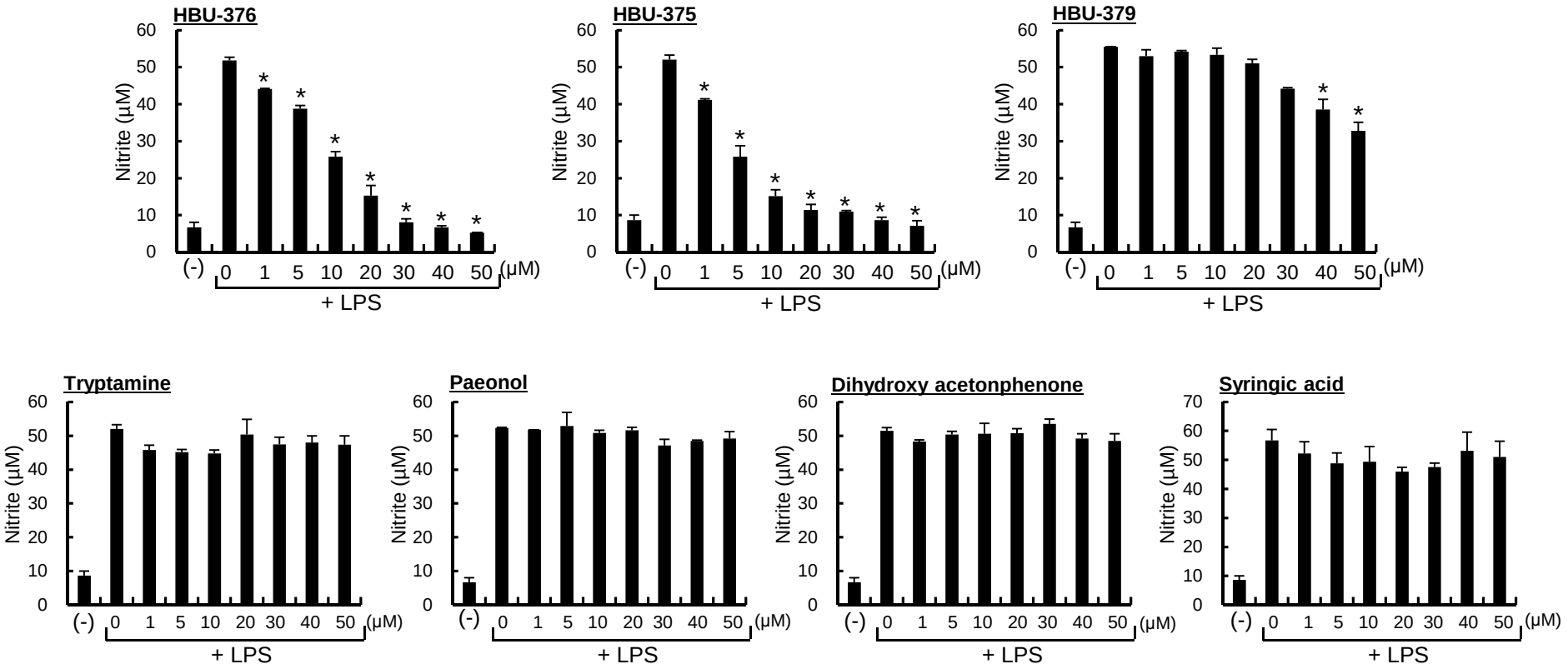
HBU-376
HBU-375
HBU-379
Tryptamine
Paeonol
Dihydroxy acetonphenone
Syringic acid
Nitrite (μM)
(-) 0 1 5 10 20 30 40 50 (μM)
+ LPS

Figure 4

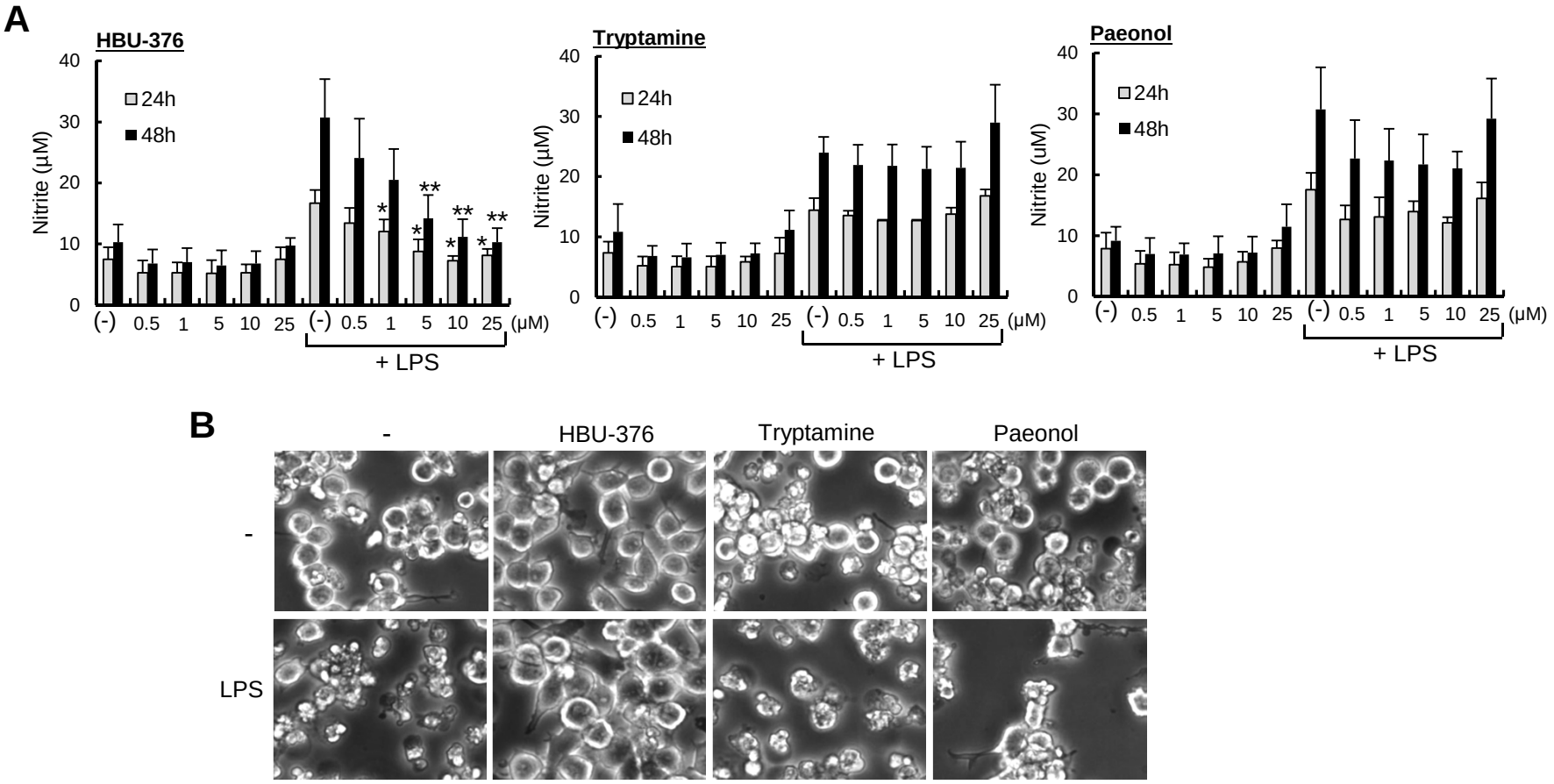
A
HBU-376
Tryptamine
Paeonol
24h
48h
Nitrite (μM)
0
10
20
30
40
(-) 0.5 1 5 10 25 (-) 0.5 1 5 10 25 (μM)
+ LPS
B
-
HBU-376
Tryptamine
Paeonol
LPS

Figure 5

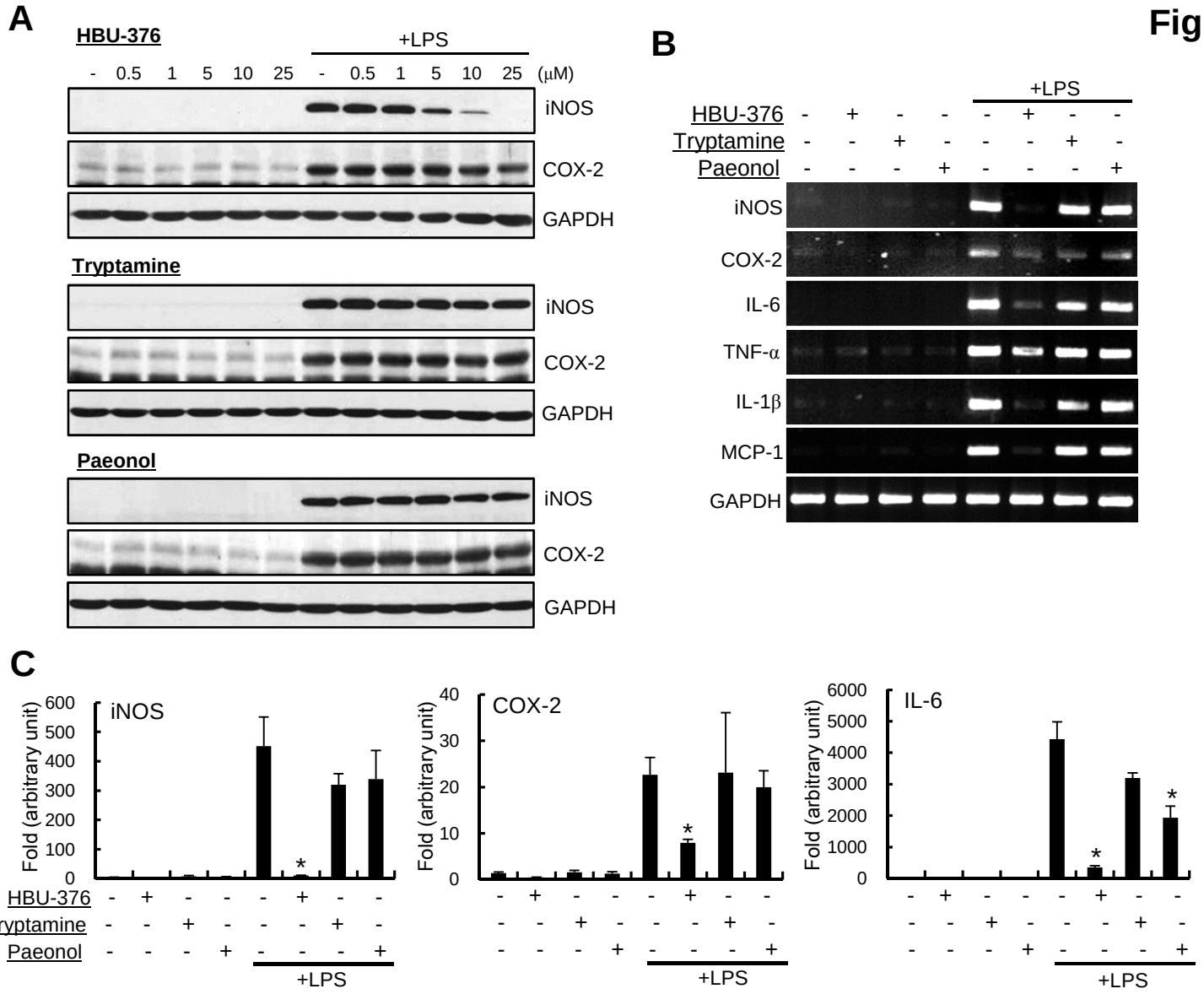
A
HBU-376
+LPS
- 0.5 1 5 10 25 - 0.5 1 5 10 25 (μM)
iNOS
COX-2
GAPDH
Tryptamine
iNOS
COX-2
GAPDH
Paeonol
iNOS
COX-2
GAPDH
B
+LPS
HBU-376 - + - - - + - -
Tryptamine - - + - - - + -
Paeonol - - - + - - - +
iNOS
COX-2
IL-6
TNF-α
IL-1β
MCP-1
GAPDH
C
iNOS
Fold (arbitrary unit)
600
500
400
300
200
100
0
HBU-376 - + - - - + - -
Tryptamine - - + - - - + -
Paeonol - - - + - - - +
+LPS
COX-2
40
30
20
10
0
IL-6
6000
5000
4000
3000
2000
1000
0

Figure 6

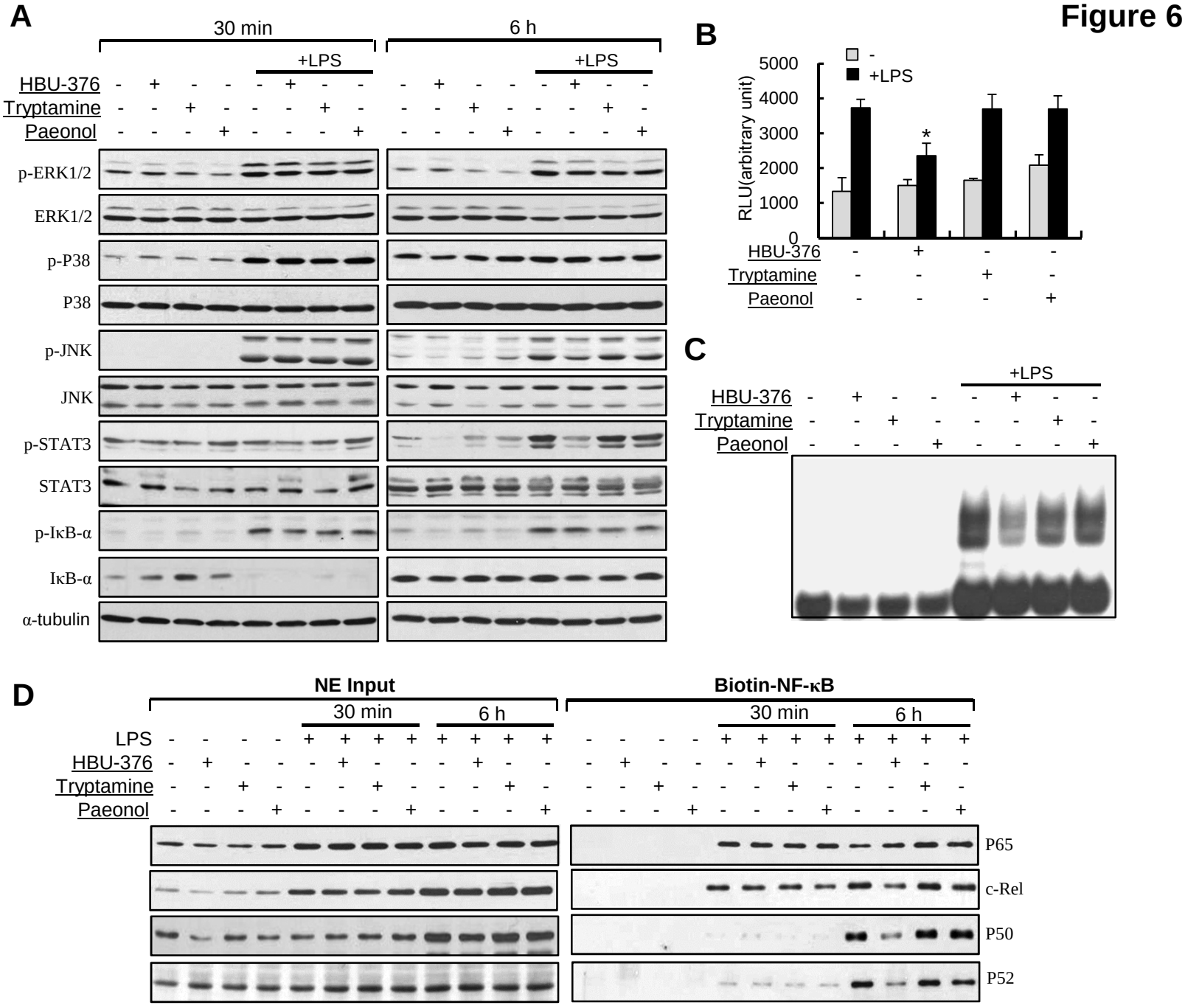
A
30 min
6 h
+LPS
+LPS
HBU-376
Tryptamine
Paeonol
p-ERK1/2
ERK1/2
p-P38
P38
p-JNK
JNK
p-STAT3
STAT3
p-IκB-α
IκB-α
α-tubulin
B
-
+LPS
RLU(arbitrary unit)
5000
4000
3000
2000
1000
0
*
HBU-376
Tryptamine
Paeonol
C
+LPS
HBU-376
Tryptamine
Paeonol
D
NE Input
Biotin-NF-κB
30 min
6 h
30 min
6 h
LPS
HBU-376
Tryptamine
Paeonol
P65
c-Rel
P50
P52

Highlights

- Tryptamine and paeonol hybridization compound (HBU-376) was synthesized.
- HBU-376 inhibited LPS-induced inflammation in BV2 cells.
- HBU-376 inhibited LPS-induced STAT-3 phosphorylation.
- HBU-376 inhibited LPS-induced NF-kappaB activation.
- HBU-376 may be therapeutic agent for inflammatory diseases of CNS.